Accepted Article

the Wnt-5a/Ca2+ pathway to antagonize Wnt/beta-catenin signaling. Mol Cell Biol 2003;23:131-139.

29. Dejmek J, Dejmek A, Safholm A, Sjolander A, Andersson T. Wnt-5a protein expression in primary dukes B colon cancers identifies a subgroup of patients with good prognosis. Cancer Res 2005;65:9142-9146.

30. Kurayoshi M, Oue N, Yamamoto H, Kishida M, Inoue A, Asahara T, Yasui W, et al. Expression of Wnt-5a is correlated with aggressiveness of gastric cancer by stimulating cell migration and invasion. Cancer Res 2006;66:10439-10448.

Acknowledgement

We thank Prof. A. Miyajima (the University of Tokyo) for the gift of anti-CK19 antibody. We thank K. Itoh, K. Okada, and A. Yanagida (Institute of Medical Science, the University of Tokyo) for excellent technical assistance.

Figure Legends

Figure 1. Expression analyses of Wnt5a and Frizzled receptors during liver development. (A) Quantitative RT-PCR analysis of Wnt5a in fetal and neonatal livers. Embryonic E14, E16, E18 and postnatal P7, and P14 indicate Wnt5a expression in whole livers derived from wild-type (WT) mice at these days of development, respectively. Values represent the ratio of Wnt5a at each stage relative to expression of this RNA in E14.5 fetal liver following normalization of template copy number to β-actin. Bars represent mean ± SD of 3 separate experiments. (B) Quantitative RT-PCR analysis of Wnt5a. Lane a, $CD45^-Ter119^-CD71^-Dlk^{high}$ cells from E14.5 liver (hepatoblasts); b, $CD45^-Ter119^-CD71^-PDGFR^+$ cells from E14.5 liver (mesenchymal cells); c: $CD45^-Ter119^-CD71^-PCLP\text{-}1^+$ cells from E14.5 liver (mesothelial cells); d, $CD45^-Ter119^-CD71^-Flk1^+$ cells from E14.5 liver (endothelial cells); e, $CD45^+Ter119^+CD71^+$ cells from E14.5 liver (hematopoietic cells). Lanes a, b, c, d, and e were normalized by numbers of β-actin copies quantified by TaqMan-PCR analysis;

Accepted Article

Accepted Article

equal numbers of copies were applied as templates. Wnt5a expression was significantly higher in mesenchymal cells than in hepatoblasts, mesothelial cells, endothelial cells and hematopoietic cells. Bars represent mean ± SD of 3 separate experiments. *$p<0.05$. (C) Expression of Frizzled (Fzd) family. Lane 1, hepatoblasts ($CD45^-Ter119^-Dlk^{high}$ cells) purified from E14.5 liver; 2, hematopoietic cells ($CD45^+Ter119^+$ cells) from E14.5 liver; 3, adult hepatocytes from 12-week-old mouse liver; 4, negative control (distilled water); 5, samples without reverse-transcriptase reaction (negative controls for false-positive amplification of genomic DNA); 6, positive control. RT-PCR products of Fzd receptors are indicated. Images shown are representative of 3 separate experiments.

Figure 2. Loss of Wnt5a excessively promotes the formation of bile duct in fetal liver. (A) Representative images depicting luminal spaces around the portal vein in E18.5 Wnt5a knock out (KO) and littermate WT livers stained with hematoxylin and eosin. (B) Quantitative RT-PCR analysis of the cholangiocyte marker Sox9 is depicted as the ratio of Sox9 copy number in E16.5 Wnt5a KO livers relative to WT livers (all normalized to β-actin). Steady-state levels of Sox9 mRNA were significantly higher in Wnt5a KO livers relative to WT livers. (C) Representative images of immunostained sections from E18.5 WT livers. Left panel; double immunostaining using CK19 (red)

Accepted Article

and entactin (green) antibodies. Right panel; double immunostaining using HNF1β (green) and HNF4α (red) antibodies. Inset black-and-white frames depict high-power-field images of cells with positive staining for CK19 (left panel) and HNF1β (right panel). (D, E) Left 2 panels; immunostaining of HNF1β (green) and HNF4α (red) in E16.5 (D) and E18.5 (E) livers. Right panel (D); number of $HNF1\beta^{+}HNF4\alpha^{-}$ cells in 10 random fields examined in WT and Wnt5a KO livers. Right panel (E); number of primitive ductal structures (PDS) in 10 random fields examined in WT and Wnt5a KO livers. (F) Left panel; immunostaining of CK19 (red) and entactin (green) in E18.5 livers. Right panel; numbers of PDS in 10 random fields of WT and Wnt5a KO livers. Arrowheads indicate PDS. Images shown are representative of 3 independent experiments. Bars in dot-plot graphs represent mean ± SEM of values shown. *$p<0.05$. **$p<0.01$. Scale bars: 50 μm.

Figure 3. Wnt5a suppresses formation of bile duct-like structures derived from hepatic stem/progenitor cells. (A) Bile duct-like branching structures derived from primary hepatoblasts. Left panel; representative view of bile duct-like branching structures consisting of >100 cells derived from primary hepatoblasts. Colonies were immunostained with CK19 (green) and counterstained with DAPI (blue). Scale bar: 100 μm. Right panel; numbers of colonies demonstrating branching structures in cultures

Accepted Article

supplemented with 100 ng/ml Wnt5a or vehicle only. Numbers of small (consisting of 10-49 cells), medium-sized (50-99 cells), and large (>100 cells) branching structures per one well were counted. (B) Numbers of bile duct-like cysts derived from the hepatic stem/progenitor cell line (HPPL) in 5 random fields per well in cultures supplemented with 100 ng/ml Wnt5a, 100 ng/ml Wnt3a, or vehicle only (left panel). There were significantly fewer small cysts (50-100 μm diameter with clear lumina) and large cysts (diameter >100 μm with clear lumina) in cultures supplemented with Wnt5a relative to vehicle only. Right panel; representative views of cysts in HPPL three-dimensional cultures supplemented with either vehicle, Wnt3a or Wnt5a. Scale bars: 50 μm. (C). Numbers of bile duct-like cysts derived from HPPL in 5 random fields per well in cultures supplemented with either control IgG, anti-Wnt5a antibody (Ab), or both anti-Wnt5a Ab plus recombinant Wnt5a protein. Cultures treated with anti-Wnt5a Ab resulted in a significant increase in total numbers of bile-duct like cysts derived from HPPL, and blocked the effect of Wnt5a supplementation. (D). Immunoblot analysis of CK19, Albumin (ALB), α-fetoprotein (AFP), and proliferating cell nuclear antigen (PCNA) in HPPL-derived cysts treated with Wnt5a. CK19 production in HPPL-derived cysts treated with Wnt5a was downregulated relative to that with vehicle-supplemented controls, whereas protein levels of ALB, AFP, and PCNA did not change. Lane 1-3 and Lane 4-6 are vehicle-supplemented controls and Wnt5a-supplemented

Accepted Article

HPPL-derived cysts, respectively. (E) Expression analysis of HPPL-derived cysts treated with Wnt5a. Expression levels of HNF1β, multidrug resistance-associated protein 3 (MRP3), and Notch1 in HPPL-derived cysts in medium supplemented with Wnt5a were significantly lower than those in HPPL-derived cysts in medium supplemented with vehicle, indicating that Wnt5a retarded biliary maturation of HPPL cysts. Results represent the mean ± SD of 3 separate experiments. *$p<0.05$. **$p<0.01$.

Figure 4. Expression of hepatic maturation markers under the culture supplemented with Wnt5a. (A) Phase contrast images of the cultured primary hepatoblasts induced to mature to hepatocytes with EHS gel alone or EHS gel plus 100 ng/ml Wnt5a. (B) Expression levels of tyrosine amino transferase (TAT), carbamoyl phosphate synthetase 1 (CPS1), tryptophan-2,3-oxygenase (TO), glucose-6-phosphatase (G6Pase), and hepatocyte nuclear factor (HNF) 4α are depicted as the ratio of copy mRNA number in cells treated with EHS gel alone or EHS gel plus 100 ng/ml Wnt5a for 7 days relative to control cells. Hc, primary adult hepatocytes (positive control). All samples were normalized by numbers of β-actin copies quantified by TaqMan-PCR analysis; equal numbers of copies were applied as templates. Results represent the mean ± SD of 3 independent experiments. *$p<0.05$.

Accepted Article

Figure 5. Inhibitors of Calcium/calmodulin-dependent kinase II (CaMKII) increased the number and size of bile duct-like cysts derived from HPPL. (A) Inhibitors specific for CaMKII activity (KN62 and KN 93) were added at the beginning of HPPL three-dimensional culture. Numbers of total cysts, small cysts and large cysts increased significantly in medium supplemented with KN62 or KN93. Cultures treated with DMSO alone (vehicle) or KN92 (an inactive analogue of KN93) served as negative controls for KN62 (vehicle) and KN93, respectively. (B) Representative DAPI-stained (blue, left panels) or phase contrast confocal microscopy images (right panels) of bile duct-like cysts. (C) Numbers of total cysts were not changed by the inhibitors of Rho kinase (Y-27632), Rac1 (NSC23766), Calcineurin (Cyclosporin A, CyA), or Protein kinase C (PKC, Go6976). Vehicle-only treatments (distilled water or DMSO) served as negative controls for Y-27632 (in distilled water), NSC23766 (in distilled water), CyA (in DMSO), and Go6976 (in DMSO). (D) Expression of multidrug resistance-associated protein 3 (MRP3) in HPPL cysts. MRP3 expression was significantly increased in medium supplemented with CaMKII inhibitor (KN62), suggesting that CaMKII inhibitor promoted biliary maturation of HPPL cysts. (E) Immunoblot analysis of CK19, AFP and PCNA in HPPL-derived cysts treated with vehicle (DMSO) or CaMKII inhibitor (KN62). The level of AFP in HPPL-derived cysts treated with CaMKII inhibitor was lower than that in vehicle-supplemented controls,

Accepted Article

whereas the levels of CK19 and PCNA did not change. Results represent the mean ± SD of 3 independent experiments. *p<0.01. **p<0.05. ***p<0.01. Scale bars: 100 μm.

Figure 6. Phosphorylation of CaMKII is regulated by Wnt5a stimulation in fetal liver. (A) Immunoblot analysis of p-CaMKII, p-PKC, and p-Rac1 in HPPL at pretreatment (0), and then 0.5, 1, 3, 6, 12, and 24 hours after stimulation by Wnt5a. Homogenate of whole E14.5 embryo served as a positive control (PTC). Wnt5a treatment increased the levels of both total CaMKII and p-CaMKII in HPPL, but did not change the levels of p-PKC and p-Rac1. (B) Representative phase-contrast images of cysts derived from HPPL supplemented either with vehicle (DMSO), 100 ng/ml Wnt5a, CaMKII inhibitor (KN62), or 100 ng/ml Wnt5a plus CaMKII inhibitor. (C) Numbers of bile duct-like cysts derived from HPPL in 5 random fields per well in cultures supplemented with vehicle (DMSO), Wnt5a, CaMKII inhibitor (KN62), or Wnt5a plus CaMKII inhibitor. The effect of Wnt5a on HPPL cysts was cancelled by KN62 treatment. (D) Immunoblot analysis of p-CaMKII in E16.5 WT and Wnt5a KO livers demonstrating a decrease in p-CaMKII level in Wnt5a KO livers. Mice 1-5 and Mice 6-10 are E16.5 WT and Wnt5a KOs, respectively. Results are represented as mean ± SD of 3 individual experiments. *p<0.05. Scale bars: 100 μm.

Accepted Article

Figure 7. Schema for the biliary differentiation of hepatoblasts in Wnt5a KO liver. Wnt5a is expressed in mesenchymal cells and other types of cells in mid-gestational fetal liver, and increases the level of CaMKII activation in hepatoblasts. The microenvironment around the portal vein, which consists of mesenchymal cells, other types of cells, and extracellular matrices, regulates appropriate differentiation of hepatoblasts into biliary cells, whereas loss of Wnt5a in such microenvironment leads to downregulation of CaMKII activation in hepatoblasts and abnormally increased formation of bile ducts.

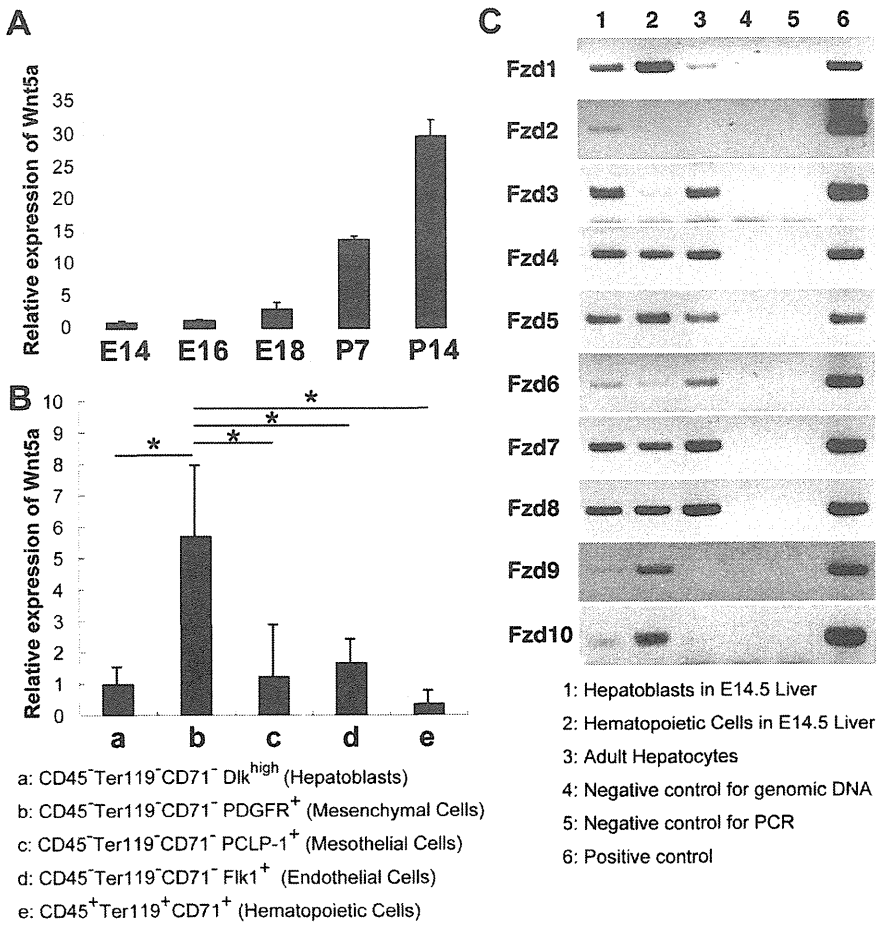

Kiyohashi *et al.* Figure 1

164x185mm (300 x 300 DPI)

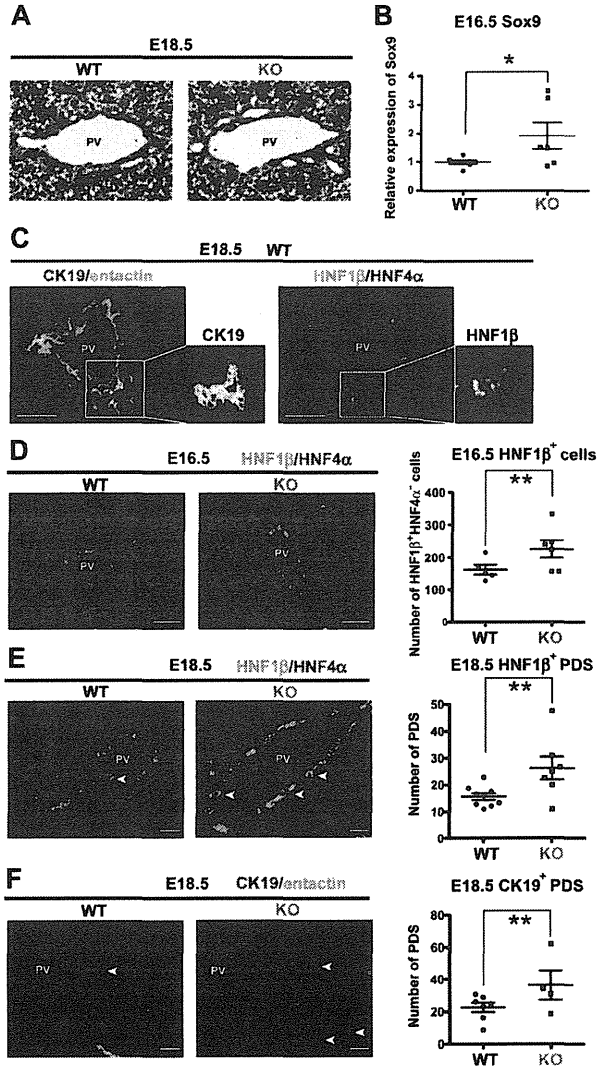

Kiyohashi *et al.* Figure 2

155x286mm (300 x 300 DPI)

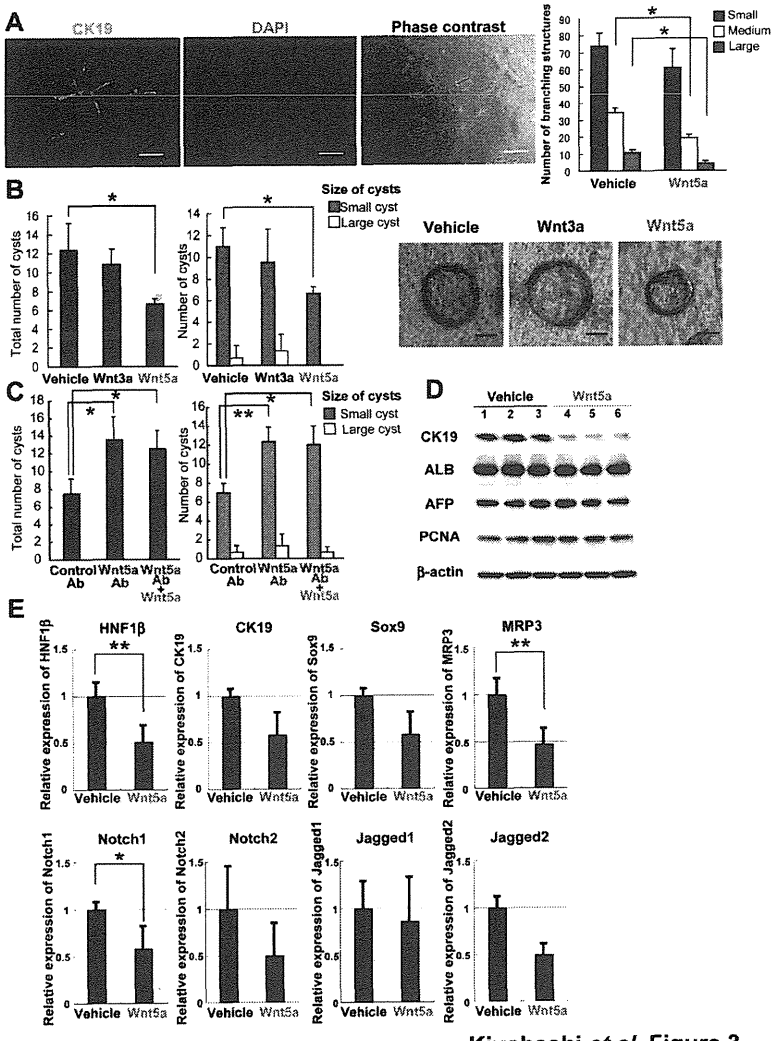

Kiyohashi *et al.* Figure 3

207x285mm (300 x 300 DPI)

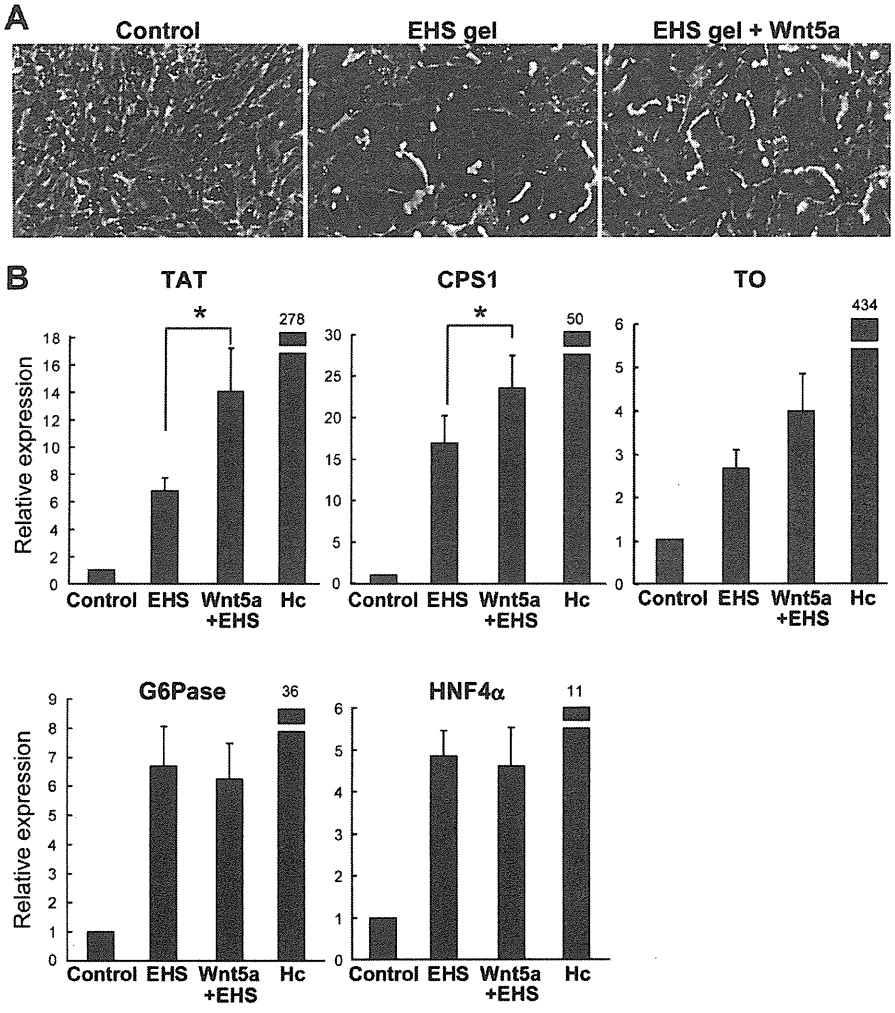

Kiyohashi *et al.* Figure 4

190x220mm (300 x 300 DPI)

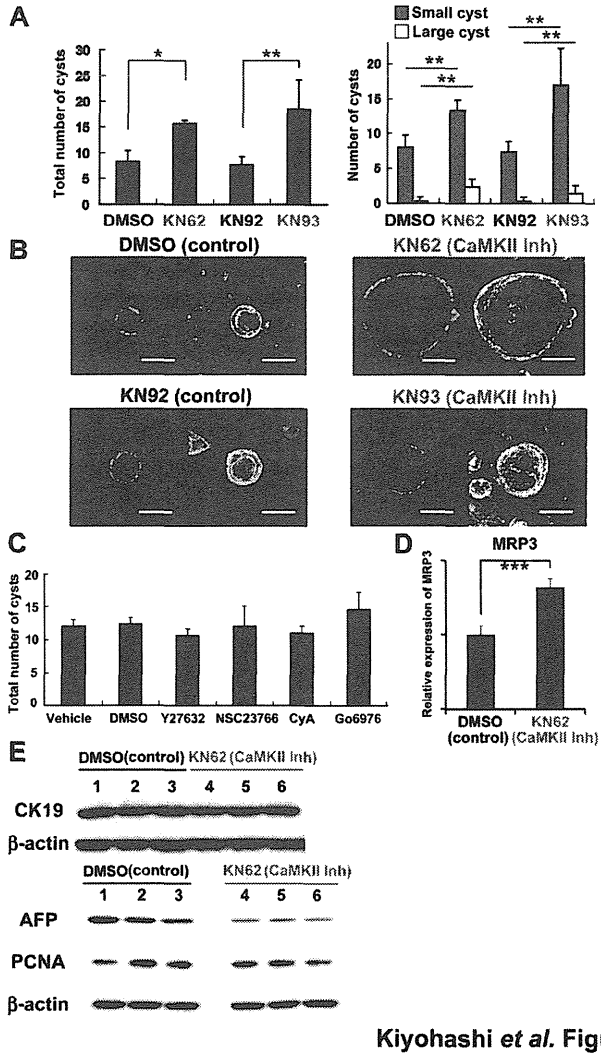

Kiyohashi *et al.* Figure 5

174x276mm (300 x 300 DPI)

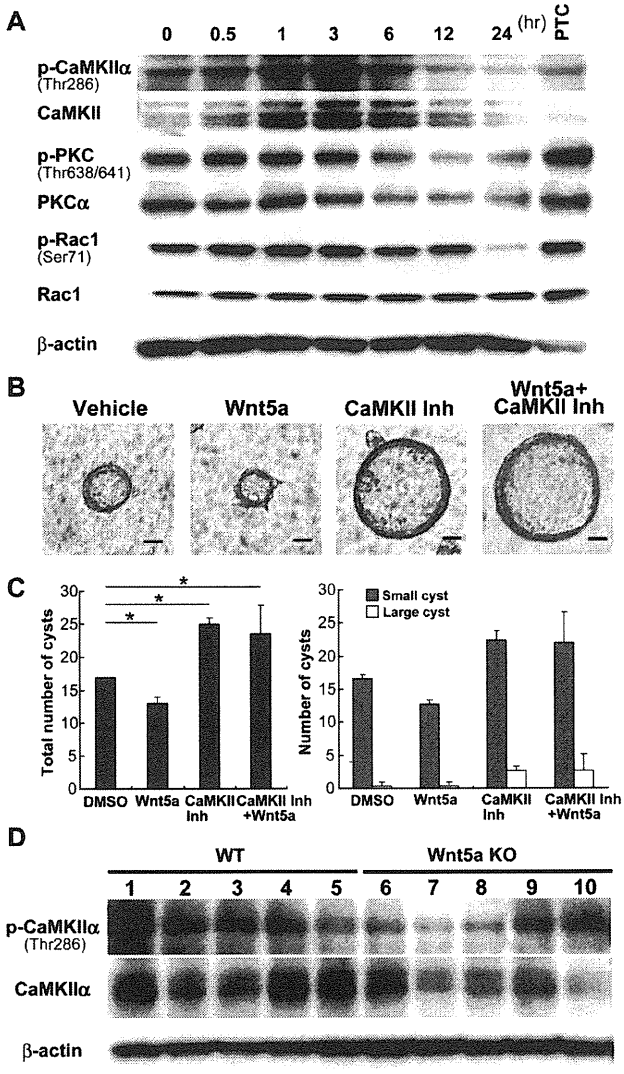

Kiyohashi *et al.* Figure 6

173x295mm (300 x 300 DPI)

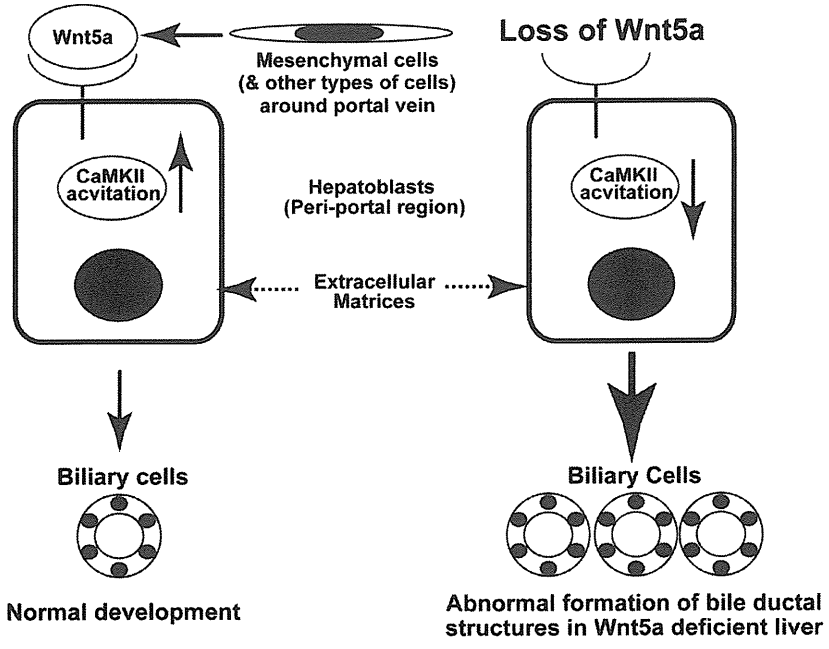

Kiyohashi *et al.* Figure 7

185x150mm (300 x 300 DPI)

Accepted

Accepted Article

Supplementary Materials and Methods

Materials.

Reagents and suppliers were: Dulbecco's modified Eagle's medium (DMEM), DMEM/F-12, fetal calf serum (FCS), penicillin/streptomycin/L-glutamine (100×), dexamethasone (Dex), non-essential amino acid solution, dimethyl sulfoxide. Sigma (St. Louis, MO); Epidermal growth factor (EGF), hepatocyte growth factor (HGF) and tumor necrosis factor (TNF) α, PeproTech (Rocky Hill, NJ); recombinant mouse Wnt3a, R&D Systems (Minneapolis, MN); recombinant mouse Wnt5a, Millipore (Billerica, MA); EHS (Engelbreth-Holm-Swarm sarcoma) gel and laminin, Becton Dickinson (Bedford, MA); 1× insulin/transferrin/selenium (ITS), Invitrogen (Carlsbad, CA); KN93 (CaMKII inhibitor), KN92 (inactive analogue of KN93), KN62 (CaMKII inhibitor), NSC23766 (Rac1 inhibitor), Y-27632 (Rho-kinase inhibitor), Go6976 (PKC inhibitor), and Cyclosporin A (calcineurin inhibitor), Calbiochem (San Diego, CA); rat anti-Dlk monoclonal antibody, Medical and Biological Laboratories (Nagoya, Japan); nicotinamide, Wako Pure Chemicals (Osaka, Japan).

Isolation of liver cells.

Fetal hepatic cells of E14.5 liver were dissociated by collagenase treatment as described.[1] Dissociated liver cells were incubated with fluorescein isothiocyanate

Accepted Article

(FITC)-conjugated anti-Dlk antibody (Ab), phycoerythrin (PE)-Cy7-conjugated anti-CD45 Ab (eBioscience, San Diego, CA), PE-Cy7-conjugated anti-CD71 Ab (eBioscience), and PE-Cy7-conjugated anti-Ter119 Ab (Pharmingen, San Diego, CA) for 60 min at 4°C. As well as with these markers, E14.5 fetal liver cells were co-stained with one of PE-conjugated anti-platelet-derived growth factor (PDGF) receptor α, PE-conjugated anti-Flk-1, and PE-conjugated anti-podocalyxin-like protein 1 (PCLP1), one Ab at a time. The stained cells were purified by use of a MoFlo™ fluorescence-activated cell sorter (FACS; DAKO, Glostrup, Denmark).

Adult hepatocyte isolation was performed following a 2-step collagenase digestion.[2] The parenchymal-cell (mature hepatocyte) fraction was separated from non-parenchymal cells by low-speed centrifugation (50 *g*, 1 min). Dead cells were removed by centrifugation in 50% Percoll solution (GE Healthcare UK Ltd, Buckinghamshire, UK); hepatocytes were then washed with PBS and collected.

Hematoxylin-eosin (HE) staining

For hematoxylin-eosin (HE) staining, liver samples were fixed in phosphate-buffered saline (PBS) containing 10% formalin for 24 h and embedded in paraffin. The samples were sectioned 5-μm thick and stained with HE.

Accepted Article

RT-PCR analysis.

The protocol for RT-PCR was previously described.[3] Briefly, total RNA samples were extracted from liver tissues with Trizol reagent (Invitrogen). For molecular analyses of HPPL-derived cysts, cells were dissociated using 0.05% collagenase solution and were collected. Then, total RNA samples were obtained using RNeasy Micro Kit (Qiagen, Hilden, Germany). First-strand cDNA was synthesized from 1 μg of RNA sample using Superscript II RNase H reverse transcriptase (Invitrogen) according to the manufacturer's instructions. The resulting cDNA samples were normalized by the number of β-actin copies (quantified by TaqMan PCR), with equal copies applied as PCR templates. The resulting cDNA was amplified using the GeneAmp PCR system 9700 (Applied Biosystems, Carlsbad, CA) at 95 °C for 3 min followed by 40 cycles at 94 °C for 10 s, 58 °C for 10 s and 72 °C for 30 s. Primers that spanned the introns of target genes were designed using the website Primer3 (http://frodo.wi.mit.edu/). Primer sequences are listed in supplementary Table 1. Amplified products were separated by electrophoresis on 1.2% agarose gels and stained with ethidium bromide.

For quantitative RT-PCR analysis, the expression of each gene was quantified using a Universal Probe Library system (Roche Diagnostics, Indianapolis, IN) and an ABI 7500 real time PCR system (Applied Biosystems). The resulting cDNA was

Accepted Article

amplified at 95 °C for 10 min followed by 40 cycles at 94 °C for 15 s and 60 °C for 60 s. Primers were designed using the website Universal Probe Library Assay Design Center (Roche). Primer sequences are listed in supplementary Table 2.

Immunohistological analysis

Protocol for immunohistological analysis was previously described.[1] Briefly, fresh livers snap-frozen in OCT compound were sectioned to 8-μm thick slices. Thawed sections were fixed in PBS containing 4% paraformaldehyde (PFA, Nakalai Tesque, Kyoto, Japan) and permeabilized using 0.1% Triton X-100/PBS. After washing with PBS, samples were incubated overnight in primary antibody (Ab; supplementary Table 3) solution at 4 °C. After washing sections 3× with PBS, they were then incubated for 60 min at room temperature in an appropriate secondary Ab solution. Microwave treatment (500 W 10 min) in 10 mM Na-citrate buffer (pH 6.0) was required for staining tissues for PCNA and Hes1. For immunostaining of PCNA, M.O.M. immunodetection kit (Vector, Burlingame, CA, USA) was used according to the manufacturer's instructions. The primary Ab against PCNA was detected using biotin-conjugated anti-mouse IgG Ab, then incubated with streptoavidin-FITC. Immunostaining of Hes1 was performed as previously described. For each analysis, addition of an appropriate immune serum provided a negative control. Nuclei were stained with 4',